Effect of "X" Ligands on the Photocatalytic Reduction of CO_2 to CO with Re(pyridylNHC-CF_3)$(CO)_3$X Complexes

Hunter Shirley, Dr. Thomas More Sexton, Dr. Nalaka P. Liyanage, C. Zachary Palmer, Dr. Louis E. McNamara, Prof. Nathan I. Hammer, Prof. Gregory S. Tschumper, and Prof. Jared H. Delcamp*

Department of Chemistry and Biochemistry
University of Mississippi
322 Coulter Hall, University, MS 38677
E-mail: delcamp@olemiss.edu
URL: www.delcampgroup.com

Supporting information for this article is given via a link at the end of the document.

Abstract: A series of five Re(pyNHC-aryl)$(CO)_3$X complexes varying the "X" ligand where pyNHC is a pyridyl *N*-heterocyclic carbene have been synthesized and characterized through NMR, UV-Vis absorption spectroscopy, IR, mass spectrometry, time-correlated single photon counting, computational analysis, and cyclic voltammetry. The photocatalytic reduction of CO_2 to CO in the presence of a sacrificial electron donor with these complexes is evaluated using a simulated solar spectrum (AM 1.5G). Comparison of Br and CH_3CN as the "X" ligand shows the same photocatalytic activity (both 32 TON). The use of Cl, NCS and $P(OEt)_3$ "X" ligands all led to diminished reactivity with as little as 2 TON for the $P(OEt)_3$ complex. These results were rationalized through computational analysis of "X" dissociation and excited-state lifetime measurements. These results highlight the importance of the "X" ligand selection on catalysis with Re-pyNHC complexes.

Introduction

Solar powered catalytic conversion of CO_2 to useable fuel precursors is an attractive avenue which could address world energy demands. CO_2-to-fuel conversion is also an ideal way to treat CO_2 waste.[1-3] Visible light absorbing photocatalysts offer the opportunity to directly reduce CO_2 to valuable fuel precursors from abundant sunlight. Homogeneous photocatalysts can be tunable and rationally modified at a molecular level; however, improvements to catalyst durability and rates of catalysis are needed for practical applications. Homogeneous photocatalysts that are effective at the direct use of sunlight without an added sensitizer are rare but offer photocatalytic CO_2 reduction with the fewest required electron transfers.[4-10] The use of a single metal complex as both the catalyst and sensitizer can significantly simplify CO_2 reduction systems relative to systems with added sensitizers which inherently require more electron transfer events.

The ligands play critical roles in the modulation of homogeneous complex reactivity, and NHC (*N*-heterocyclic carbene) ligands often give homogeneous catalysts with increased durability.[11] Furthermore, the strong electron donating properties of these ligands to the metal center may assist in enhancing the performance of reductive catalysis. In fact, we recently demonstrated pyridyl-NHC (pyNHC) ligated Re-complexes such as (Re(pyNHC-$PhCF_3$)$(CO)_3$Br (**2**) could directly photocatalyze the reduction of CO_2 to CO at rates surpassing the well-known Re(bpy)$(CO)_3$Br (**1**) benchmark photocatalyst (Figure 1).[5-6] A significant increase in durability of the Re(pyNHC-$PhCF_3$)$(CO)_3$X catalyst is also observed relative to

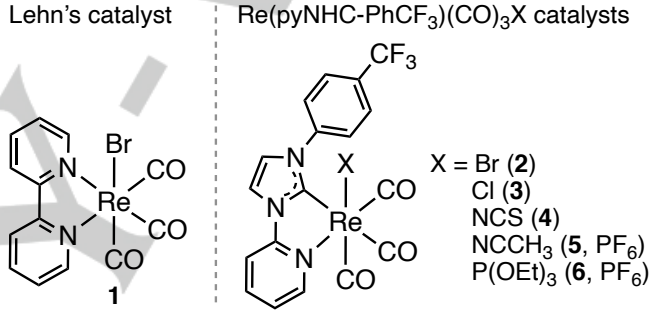

Figure 1. Structures of the first reported rhenium photocatalyst (**1**) and the Re(pyNHC-$PhCF_3$)$(CO)_3$X photocatalysts studied in this work with varied "X" groups (**2**-**6**).

the benchmark when electron deficient aryl groups were evaluated with "X" as bromide (**2**) rather than chloride (**3**).

Mechanistically, it is believed that photoexcitation results in a metal-to-ligand charge transfer (MLCT) followed by reduction and dissociation of a rhenium ligated "X" group to give an open coordination site (Figure 2).[12-13] Other notable photochemical pathways have also been proposed including direct photodissociation of the X group prior to reduction or CO photodissociation prior to the X group.[14-15] Computationally, an elongation of the Re-Br bond upon reduction of catalyst **2** is reported.[5] With these results in mind, the coordination strength of the monodentate ligand could play an important role in the rate of opening a coordination site to give an active catalyst, which may affect overall catalysis rates for these complexes similar to Re(bpy)$(CO)_3$X complexes.[16] This study focuses on understanding the effects of varying the monodentate "X" ligand on catalyst behavior.

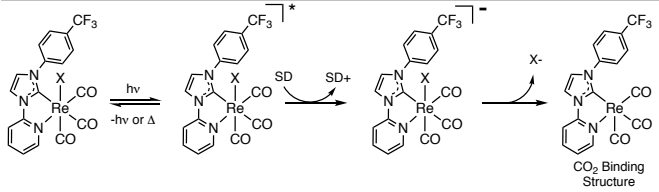

Figure 2. Initial catalytic cycle steps illustrated with a Re(pyNHC-PhCF$_3$)(CO)$_3$X catalyst.

Concerning the Re(pyNHC-PhCF$_3$)(CO)$_3$X complex "X" ligand, a significant change in photocatalytic performance was previously observed when bromine complex **2** is compared with the chloride complex **3**.[6] Thus, a series of complexes varying the rhenium bromide substituent of **2** was targeted. Pseudo halide-based NCS (isothiocyanate) complex **4** was targeted for photocatalytic studies in addition to non-anionic ligands with PF_6 counter ions such as weakly coordinating MeCN (**5**) and stronger coordinating P(OEt)$_3$ (**6**). Herein, the catalysts properties are analyzed via absorption spectroscopy, emission spectroscopy, cyclic voltammetry, photocatalytic performance studies, computational analysis, and excited-state lifetime studies.

Results and Discussion

The syntheses of the Re(pyNHC-PhCF$_3$)(CO)$_3$X complexes **2** and **3** are reported in literature.[6, 17] Catalyst **2** was used to synthesis complexes **4**-**6** through simple metathesis reactions with either sodium or silver salts (Scheme 1). Catalyst **4** was synthesized in good yield (65%) in a single step by reacting **2** with NaNCS under reflux. The synthesis of catalysts **5** is a single step metathesis reaction of **2** and silver hexafluorophosphate in acetonitrile (MeCN) in 86% yield. Finally, complex **6** was synthesized by first reacting catalyst **2** with silver triflate in tetrahydrofuran (THF) to presumably give a THF-complex. The complex was then reacted directly with triethyl phosphite, and the counter ion was exchanged to hexafluorophosphate analogous to prior reports to give the desired product in 59% yield.[12] All complexes were characterized via ^{1}H NMR, ^{13}C NMR, ^{19}F NMR, infrared spectroscopy, and high resolution mass spectrometry before the electrochemical and photophysical studies were conducted below.

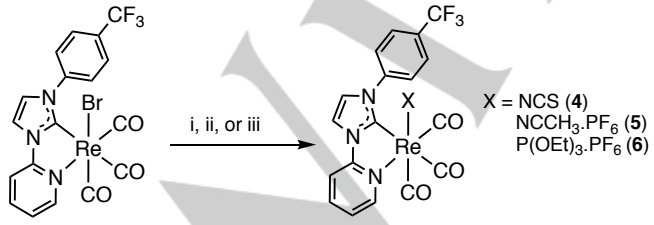

Scheme 1. i) NaSCN, ethanol:water (1:1) reflux, **4**: 65% yield. ii) $AgPF_6$, MeCN, **5**: 86% yield. iii) $AgSO_3CF_3$, THF, reflux; P(OEt)$_3$, reflux; NH_4PF_6 (MeOH), **6**: 59% yield.

With the desired complexes in hand, the effects of "X" group on complex energetics were first analyzed via absorption spectroscopy, emission spectroscopy, and cyclic voltammetry measurements. Complexes baring an anionic "X" ligand (**2**, **3**, and **4**) have very similar absorption spectrum with low energy maximum absorption peak (l_{max}) peaks narrowly ranging from 350-356 nm with molar absorptivities (e) of 4,400-4,900 $M^{-1}cm^{-1}$ (Figure 3, Table 1). All three complexes show a lower energy shoulder at approximately 400 nm (e = 1,200-1,400 $M^{-1}cm^{-1}$) which is attributed to the metal-to-ligand charge transfer (MLCT) absorption feature based on the reported literature.[5] All of these complexes show absorption onsets reaching values >425 nm which indicates they can use visible light to drive photocatalytic reactions. When the "X" ligand is neutral (**5** and **6**), the l_{max} and the associated low energy shoulder feature shift to higher energy absorption by approximately 30-40 nm relative to **2**-**4** with similar e values. This shift is expected due to the reduction

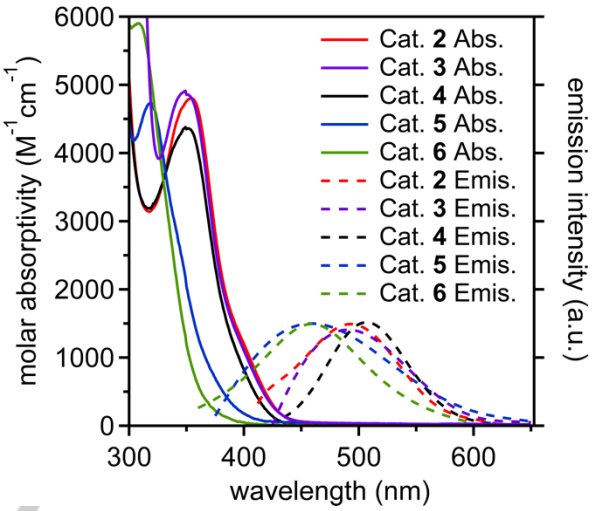

Figure 3. UV-Vis absorption and emission spectra of catalyst **2**-**6**. All data were collected in MeCN and the emission is normalized.

of electron density on the Re center with the cationic complexes which leads to a higher energy being needed to facilitate an MLCT event. For these two complexes the absorption curve onsets reach 400 nm, which is the beginning of the visible spectrum. As a result, these two complexes are expected to have few excited states during photolysis.

The emissive properties of the complexes were measured to find the energy of the absorption and emission curve intercept ($E_{(MLCT-GS)}$, where GS is the ground-state). All of the complexes were weakly emissive with the anionic "X" complexes showing emission maxima (λ_{em}) from 495-504 nm and $E_{(MLCT-GS)}$ values from 2.88-2.97 eV (Figure 3, Table 1). The complexes with a neutral "X" ligand gave higher energy emission maxima at 452-455 nm and higher energy $E_{(MLCT-GS)}$ from 3.22-3.44 eV. The excited-state lifetimes of the complexes were measured to ensure the excited state are persistent enough to allow for electron transfers to take place. A range of lifetimes were observed from 2.8 ns to 15.4 ns for **2**-**6** in N_2 degassed MeCN. The change in lifetime based on X is consistent with prior literature reports.[18] The shortest lifetimes were observed for the cationic complexes **5** and **6** with neutral "X" ligands at 2.9 ns and 2.8 ns, respectively.

The bromide ligated **2** had the shortest lifetime among the anion "X" ligated complexes at 4.3 ns. The chloride and NCS ligated complexes had significantly longer lifetimes at 12.2 ns and 15.4 ns, respectively. The lifetimes of the NHC complexes were shorter than the bipyridyl benchmark **1** at 50 ns;[5] however, all of these complexes are kinetically competent to undergo diffusion-based bimolecular electron transfer events.

The ground state reduction potentials ($E_{(S/S-)}$) and excited state reduction potentials ($E_{(S^*/S-)}$) can be approximated via cyclic voltammetry (CV) measurements with $E_{(MLCT-GS)}$ values for each complex. Due to the irreversible reduction reactions of these complexes, thermodynamic comparisons are approximated from

Table 1. Photochemical and electrochemical data in MeCN.

cat.	λ_{max} (nm) peak | sh[a]	ε ($M^{-1}cm^{-1}$) peak | sh[a]	λ_{em} (nm)	τ (ns)	$E_{(MLCT-GS)}$ (eV)[b]	$E_{(S/S-)}$ (V)[c] onset | peak	$E_{(S^*/S-)}$ (V)[d]	i_{cat}/i_p red. 1	i_{cat}/i_p red. 2
2	356 | 400	4800 | 1400	496	4.3	2.97	–1.90 | –2.05	0.92	1.6	2.0
3	350 | 400	4900 | 1400	495	12.2	2.88	–1.94 | –2.11	0.77	1.8	2.1
4	352 | 400	4400 | 1200	504	15.4	2.87	–1.97 | –2.14	0.73	2.0	2.0
5	320 | 350	4700 | 2900	455	2.9	3.22	–1.74 | –1.85	1.37	2.6	4.8
6	310 | 340	5800 | 2800	452	2.8	3.44	–2.02 | –2.14	1.30	1.0	1.8

[a] Shoulder. [b] $E_{(MLCT-GS)}$ (nm) was taken from the crossing point of absorption and emission curve and was converted to eV via the equation: $E_{(MLCT-GS)}$ (eV) = 1240/$E_{(MLCT-GS)}$ (nm). [c] Measured via cyclic voltammetry under argon in MeCN with 0.1 M Bu_4NPF_6, 1.0 mM catalyst, and using ferrocene as an internal standard, Pt as the counter electrode, Pt wire as the pseudo-reference electrode, and glassy carbon as the working electrode. [d] Calculated using the following equation $E_{(S^*/S-)} = E_{(MLCT-GS)} + E_{(S/S-)}$ with the peak potential value for $E_{(S/S-)}$.

the onset potentials whereas the peak potentials may shift due to undetermined chemical reactions. The reduction potentials at both the onset of reduction and peak reduction were found in the following order from more positive (easier to reduce) to more negative (harder to reduce): **5** > **2** > **3** > **4** > **6** (Table 1, Figure 4). Interestingly, the two neutral "X" complexes were found to have the most and least negative $E_{(S/S-)}$ onset values of the series at –1.74 V and –2.02 V versus ferrocenium/ferrocene (Fc^+/Fc). The relatively easily reduced complex **5** was expected to reduce most easily given that the Re-complex is cationic with a weakly donating "X" ligand. The bromide complex **2** is the next most easily reduced complex at –1.90 V which can be explained by bromide providing the least electron density to the Re metal center. The chloride and NCS complexes are similar in reduction potential at –1.94 V and –1.97 V. The hardest to reduce complex uses a $P(OEt)_3$ ligand which is strongly electron donating. Notably, all of these complexes are energetically favorable for the reduction of CO_2 to CO at the first reduction potential even when considering the wide possible reduction potential range of CO_2 (–0.90 V to –0.12 V) since the pK_a of the strongest acid in the photoreactions studied is not known (Figure 5).[19] The most easily reduced complex **5** would still have an estimated minimum free-energy for electron transfer to CO_2 of 840 mV at the first reduction wave onset.

To ensure an adequate sacrificial electron donor (SED/SD) is selected, the $E_{(S^*/S-)}$ values must be analyzed. From the equation $E_{(S^*/S-)} = E_{(MLCT-GS)} + E_{(S/S-)}$, the $E_{(S^*/S-)}$ values were estimated to range widely from 0.73 V to 1.37 V based on reduction peak potentials (Table 1). Notably the anionic "X" complexes have the least positive $E_{(S^*/S-)}$ values at 0.73-0.92 V. The neutral "X" ligated complexes are significantly more positive in $E_{(S^*/S-)}$ values at 1.30-1.37 V. This is expected since the cationic complexes would have more stabilized electrons on the Re center being photoexcited during the MLCT event leading to a more potent oxidant. For the photocatalytic experiments studied herein, 1,3-dimethyl-2-phenyl-2,3-dihydro-1H-benzo[d]imidazole (BIH) is used as the SED with a potential of –0.10 V for an estimated minimum free energy of electron transfer at 830 mV for the NCS complex **4** (Figure 5). Even though the $E_{(S^*/S-)}$ values are only estimates, the driving force for electron transfer is substantial and favorable in all cases. This indicates favorable electron transfer energetics can be expected with these catalysts when powering the photoinduced reduction of CO_2 with BIH as an SED. Additionally, the catalytic reduction was briefly analyzed by obtaining CVs under CO_2 and comparing these to CVs under N_2 to observe current changes. Under CV conditions, catalysts **2**-**5** all show 1.6-2.6 times increase in current under CO_2 at the first reduction wave according to the trend: **2** < **3** < **4** < **5**. Catalytic activity at the first reduction wave during CO_2 reduction is well documented in the literature for NHC ligated complexes.[6, 17, 20-24] Notably, complex **6** and benchmark **1** show negligible current changes at the first reduction wave with catalytic reactivity occurring at the second reduction wave.[6] Importantly, all of the complexes show catalytic behavior toward CO_2 electrochemically, which encourages the further study of these complexes in a photocatalytic system.

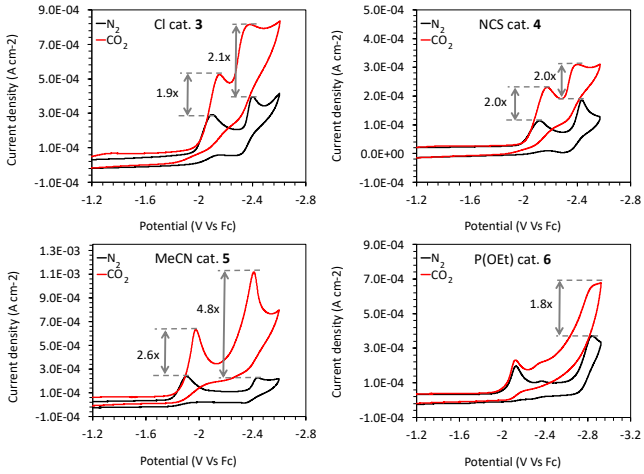

Figure 4. CV curves for the catalysts **4-6,** measured in acetonitrile with 0.1 M *n*-Bu_4NPF_6 electrolyte under N_2 (black) and CO_2 (red) atmosphere. Glassy carbon working electrode, platinum counter electrode, and platinum pseudo-reference electrodes are with ferrocene as an internal standard and a scan rate of 100 mV/s. All potential values are reported versus Fc^+/Fc.

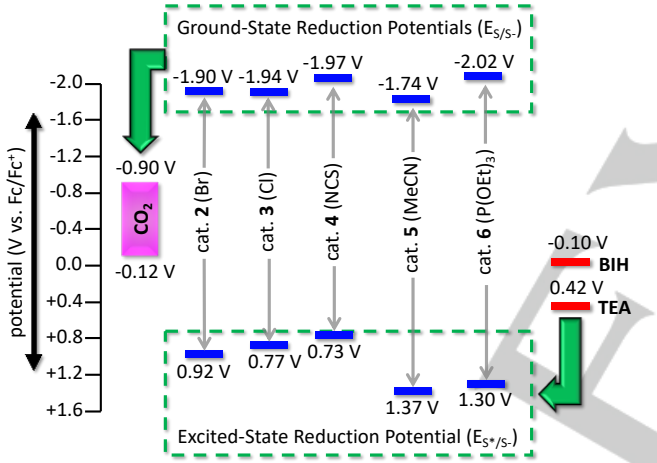

Figure 5. Energetic diagram for each complex relative to CO_2 and SEDs.

Photocatalytic studies were undertaken with each catalyst in MeCN with BIH as a sacrificial electron donor and triethylamine (TEA) to react with BIH^+ to promote irreversible electron transfers from BIH to the catalysts (Table 2, Figure 6). The reactions were run under a CO_2 atmosphere with irradiation from a solar simulated AM 1.5G spectrum at 1 sun intensity. Under these conditions Re(bpy)$(CO)_3$Br (**1**) gives 14 turnovers (moles of CO/moles of catalyst) at a turnover frequency (TOF, TON/time) of 25 h^{-1} (Table 2, entry 1). Re(pyNHC-$PhCF_3$)$(CO)_3$Br (**2**) was found to be twice as durable at 32 TON and approximately twice as fast at 48 h^{-1} which is a result of the stronger binding NHC group with increased donation strength (Table 2, entry 2). Exchange of the Br for Cl (complex **3**) resulted in a lower TON (22) and a lower TOF (33 h^{-1}) complex (Table 2, entry 3). Similarly, Re(pyNHC-$PhCF_3$)$(CO)_3$NCS (**4**) gave 20 TON and a TOF of 32 h^{-1} (Table 2, entry 4). Thus, among the anionic "X" ligand catalysts, the bromide ligated complex was the most durable and the fastest catalyst. Given that the first chemical step toward accessing an active catalyst species is "X" ligand dissociation and reassociation of "X" to an active catalyst species would likely only hinder catalysis, the Re-Br bond is likely the weakest among the series with a similar binding strength of Re-Cl and Re-NCS. $[Re(pyNHC\text{-}PhCF_3)(CO)_3MeCN]^+$ (**5**) shows a similar TON (31) to Re(pyNHC-$PhCF_3$)$(CO)_3$Br with a higher TOF of 60 h^{-1} indicating the weakly bound MeCN neutral ligand behaves similarly to the anion Br ligand during catalysis which suggests that bromide is a weak ligand in this system (Table 2, entry 5). The $[Re(pyNHC\text{-}PhCF_3)(CO)_3P(OEt)_3]^+$ complex (**6**) shows very low reactivity at only 2 TON and a TOF of 5 h^{-1} (Table 2, entry 6) which suggest the $P(OEt)_3$ ligand does not readily dissociate. A series of control experiments removing CO_2, BIH, or catalyst reveals all components to be necessary for catalysis (Table 2, entries 7-9).

Introduction of Br^- or Cl^- to the reaction mixture as a tetrabutylammonium (TBA) salt with Re(pyNHC-$PhCF_3$)$(CO)_3$Br (**2**) led to a lower TON (25 or 27 relative to 32 with no added salt) and a lower TOF (30 or 45 relative to 48 h^{-1} with no added salt) (Table 2, entries 10-11). This lower performance is expected if the anionic ligand is involved in any deactivation pathways resulting from association of the ligand to an active catalyst species. To examine the effects of TBA on catalysis in the absence of added coordinating anion, $TBAPF_6$ was added to the reaction mixture resulting in highest TON observed in these studies at 40 and the

Table 2. TON and TOF values of photocatalysts with and without additives.

Entry	Complex	Change[a]	CO TON	TOF [b] (h^{-1})
1	**1**	none	14	25
2	**2**	none	32	48
3	**3**	none	22	33
4	**4**	none	20	32
5	**5**	none	31	60
6	**6**	none	2	5
7	**2**	+N_2, –CO_2	1	--
8	**2**	–BIH	1	--
9	none	none	0	--
10	**2**	+TBABr	25	30
11	**2**	+TBACl	27	45
12	**2**	+$TBAPF_6$	40	51

[a] Standard conditions (0.1 mM catalyst, 10 mM BIH, 350mM TEA, CO_2, MeCN, 1 sun intensity solar simulated spectrum at AM1.5) were used unless otherwise noted. Note: The concentration of BIH is limited by solubility in MeCN with a maximum of 100 TON possible with this system assuming BIH transfers 2 electrons and TEA transfers no electrons.[25] The highest TON reaction accounts for less than 1/2 of the total possible TON possible based on sacrificial electron donor amounts. [b] TOF is measured after 20 minutes of photocatalysis.

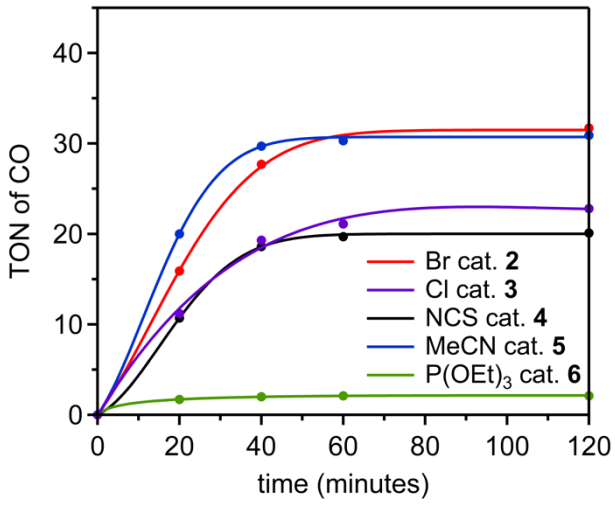

Figure 6. Turnover number versus time plot for CO production. Data points are the average of two runs.

highest TOF in these studies at 51 h^{-1} (Table 1, entry 12). This may be due to increasing the ionic strength of the solution which could promote Br^- dissociation from Re(pyNHC-PhCF$_3$)(CO)$_3$Br (**2**). Given that TBA is catalyst performance enhancing, the diminished TON values observed with TBABr and TBACl indicates a significantly deleterious effect of the anions on catalysis. These results are distinctly different to those originally reported with Re(pyNHC-PhCF$_3$)(CO)$_3$Br (**1**) and Re(pyNHC-PhCF$_3$)(CO)$_3$Cl (**3**) where tetraethylammonium perchlorate has no effect on catalysis and tetraethylammonium chloride shows higher catalyst performance.[4]

Computational studies at the M06-L/aug-cc-pVTZ-PP and M06-2X/aug-cc-pVTZ-PP levels of theory were undertaken to better understand the role of the "X" ligands on catalysis (Table 3). Zero-point vibrational energy (ZPVE) corrected dissociation energies (D_0) were computed with a polarizable continuum model (PCM) of acetonitrile. For the anionic "X" ligated complexes, the 1 electron reduced complex was used as the ligand associated complex. For the neutral "X" ligated complex, the neutral complex was used as the associated complex which allows for all of the complexes to give the same charge ligand dissociated complex. The CF$_3$ group on the pyNHC-PhCF$_3$ ligand was truncated to H to reduce computational demands. Notably, Re(pyNHC-Ph)(CO)$_3$Br is known to be catalytically competent at near the same TON values as the benchmark Re(bpy)(CO)$_3$Br.[6] P(OMe)$_3$ was included in the computational analysis to prove the effect of a phosphite ligand with a reduced steric environment relative to P(OEt)$_3$. M06-2X shows the anticipated trend for dissociation energies ranging from 3.1-13.6 kcal/mol where: MeCN < Br^- < Cl^- < NCS^- < P(OEt)$_3$ < P(OMe)$_3$ (Table 3). This trend loosely correlates with the observed TOF reactivity trend in Figure 6; however, the energetic value changes are not proportional to the TOF value changes. Correlation to the TOF values is possible if anion association/dissociation steps are in equilibrium; however, given that the magnitude of changes are not proportional to the binding energies, alternate roles of the X group could be possible beyond simple dissociation/association paths from the parent complexes or explicit solvent interactions may be needed to more accurate predict the dissociation energies. Specifically, it is not obvious why the NCS^- ligand has a dissociation energy nearly double that of Cl^-, but has a similar TON and TOF. M06-L shows a similar trend to M06-2X with the only change being a smaller D_0 for Br^- than MeCN. Comparatively to Re(bpy)(CO)$_3$Br, Re(pyNHC-Ph)(CO)$_3$Br shows a 7.9 kcal/mol lower D_0 with the M06-2X level of theory. With such a higher D_0 value it would be expected that the Br^- ligand would not readily dissociate from $[Re(bpy)(CO)_3Br]^-$ but dissociation from $[Re(pyNHC\text{-}PhCF_3)(CO)_3Br]^-$ should be facile at 3.1 kcal/mol. To probe this hypothesis, CVs were acquired where the switching potential was set at approximately 0.1 V more negative than the peak reduction potential for each complex (Figure 7). On a CV timescale with a sweep rate of 100 mV/s, Re(bpy)(CO)$_3$Br shows reversibility at the first reduction wave indicating that the chemical step of "X" dissociation occurs at a slower rate than observed with this measurement. However, on a CV timescale, the "X" group on Re(pyNHC-PhCF$_3$)(CO)$_3$Br was found to completely dissociate with no evidence of reversibility. Increasing the scan rate from 100 mV/s to 9 V/s shows no evidence of reversibility which further supports that the Br^- dissociation from Re(pyNHC-PhCF$_3$)(CO)$_3$Br is facile (Figure S1). This observation is consistent with the computational findings and explains the difference observed in reactivity via CV for each of the complexes with Re(pyNHC-PhCF$_3$)(CO)$_3$Br showing CO_2 reduction reactivity on the first reduction wave while catalytic reactivity is not observed until the second reduction wave for Re(bpy)(CO)$_3$Br. Re(pyNHC-PhCF$_3$)(CO)$_3$P(OEt)$_3$

Table 3. Zero-point vibrational energy (ZPVE)[a] corrected dissociation energy (D_0, in kcal/mol) for various ligands in the PCM acetonitrile computed with aug-cc-pVTZ-PP at aug-cc-pVDZ-PP optimized geometries.

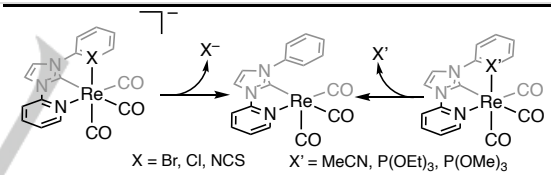

	M06-L/aug-cc-pVTZ-PP[a]	M06-2X/aug-cc-pVTZ-PP[a]
	Re(pyNHC-Ph)(CO)$_3$X	
Br^-	3.7	3.1
Cl^-	4.8	4.4
NCS^-	10.3	8.5
MeCN	4.6	3.0
P(OEt)$_3$	13.2	12.5
P(OMe)$_3$	14.8	13.6
	Re(bpy)(CO)$_3$Br	
Br^-	9.6	11.0

[a] ZPVE from unscaled aug-cc-pVDZ-PP harmonic vibrational frequencies for each method.

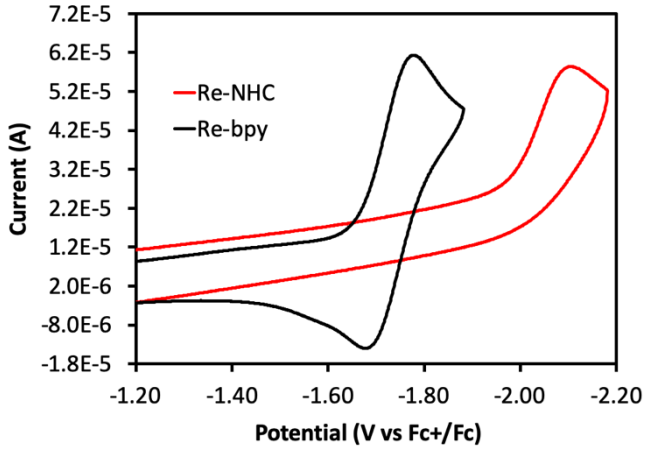

Figure 7. Cyclic voltammograms for Re(pyNHC-PhCF$_3$)(CO)$_3$Br and Re(bpy)(CO)$_3$Br with a switching potential at 0.1 V past the reduction peak with a scan rate of 100 mV/s.

shows a similar behavior to Re(bpy)(CO)$_3$Br in that neither complex shows catalytic reactivity at the first reduction wave and both have high calculated D_0 values relative to the remaining complexes studied.

Conclusion

Five Re(pyNHC-PhCF$_3$)(CO)$_3$X complexes were synthesized and characterized. Absorption spectroscopy shows a significant red shift when "X" is an anionic ligand versus a neutral ligand. Additionally, emissive excited state lifetime studies reveal that the anionic ligated complexes have longer excited state lifetimes at up to 15.4 ns. The weakly coordinated MeCN complex was found to have the least negative reduction potential followed by the anionic "X" ligated complexes closely grouped in reduction potential values. All of the complexes studied except Re(pyNHC-PhCF$_3$)(CO)$_3$P(OEt)$_3$ (**6**) show catalytic reactivity at the first reduction wave for the 2-electron reduction of CO_2. The photocatalytic CO_2 reduction reaction rates loosely correlate to the calculated bond dissociation energies, albeit not proportionally. The highest reactivity for both photocatalysis and electrocatalysis was observed with when "X" is MeCN with a comparable reactivity with the Br complex in the photocatalytic system. MeCN and Br^- also have the two lowest bond dissociation energies calculated. The bond dissociation energy is calculated to be significantly higher when a bpy ligand is used in place of the pyNHC ligand, and this prediction is supported by CV evidence showing a rapid dissociation of Br^- from Re(pyNHC-PhCF$_3$)(CO)$_3$Br with a slow dissociation of Br^- from Re(bpy)(CO)$_3$Br. These results aid in explaining the empirically observed reactivity differences between pyNHC and bpy ligated complexes in CO_2 reduction literature. Additionally, these results also highlight the importance of controlling the "X" ligand composition since it has a clear effect on catalysis despite the "X" dissociation step being outside the catalytic cycle. This suggests the "X" group is part of reversible association/dissociation pathways that deactivate/activate catalytically competent intermediates during CO_2 reduction reactions. This study will aid in guiding future catalyst designs focused on NHC catalyst preparation, "X" ligand selection, and catalytic condition selection where coordinating "X" ligands should be avoided for maximal reactivity.

Experimental Section

General Information. All commercially obtained reagents were used as received except MeCN which was freshly distilled before use over calcium hydride. Unless, otherwise noted, all the reactions were conducted under a CO_2 atmosphere. Thin-layer chromatography (TLC) was conducted with sigma T-6145 pre-coated TLC silica get 60 F_{254} polyester sheets and visualized with 254 nm light. Flash column chromatography was performed with SilicaFlash P60, 40-63 μm (230-400 mesh). ^{1}H NMR spectra were recorded on a Bruker Avance DRX-500 (500 MHz) spectrometer and reported in ppm using solvent as an internal standard ($CDCl_3$ at 7.26 ppm for ^{1}H NMR and 77.23 ppm for ^{13}C NMR or CD_3CN at 1.94 ppm for ^{1}H NMR and 118.26 ppm for ^{13}C NMR). Data reported as: s = singlet, d = doublet, t = triplet, q = quartet, p = pentet, m = multiplet, b = broad, ap = apparent; coupling constants in Hz. FT-IR samples were run on a Bruker Alpha ATIR spectrometer. UV-Vis spectra were collected on a Cary 5000 spectrometer. Emission spectra were collected using a PerkinElmer LS55 Fluorescence Spectrometer. Samples for emission studies were degassed with N_2 prior to collecting spectrum in acetonitrile. Cyclic voltammetry was performed using a CH Instruments potentiostat (CHI-600E) with a glassy carbon electrode as the working electrode, platinum as the counter electrode, and platinum as the pseudo-reference electrode with ferrocene as an internal reference. 0.1 M *n*-Bu_4NPF_6 is used as the supporting electrolyte and all the measurements were taken in acetonitrile. 3.0 ml of electrolyte solution at 1.0 mM catalyst concentration was used in each experiment. Before each measurements the electrolyte solution was degassed with N_2 or CO_2 (~15 min). To avoid changes in concentration during degassing, pure acetonitrile was first added to the electrolyte solution (~5 mL) and the solution was degassed until the final volume was reduced to 3.0 ml. CV measurements were taken at a scan rate 100 mV/s^{-1} and the sweep width window was set to ~100 mV past the second reduction potential for each catalyst. A 150 W Sciencetech SF-150C small collimated beam solar simulator equipped with an AM 1.5 G filter was used as the light source for the photocatalytic experiments. Head space analysis was performed using gas tight valved syringes to extract the sample and analysis was performed with a custom Agilent 7890B gas chromatography instrument equipped with an Agilent PorapakQ 6ft, 1/8 O.D. column. Quantitation of CO and CH_4 were made using an FID detector, while H_2 was quantified using a TCD detector. In these studies, CO was the only appreciable product detected. All GC calibration standards were purchased from BuyCalGas.com. For excited-state lifetime measurements, all sample concentrations were on the order of 10^{-5} M to reduce reabsorption. Fluorescent lifetimes were obtained by exciting with a Picoquant LDH-P-C-405B 405 nm diode laser (fwhm < 100 ps) and detecting with a PDM series single photon avalanche diode (Micro Photon Devices, Bolzano, Italy). Complexes **1**-**3** are previously reported.[6, 17] 1,3-dimethy-l-2-phenyl-2,3-dihydro-1H-benzo[d]imidazole (BIH) was prepared as previously reported.[6]

Synthesis. *Fac*-(3-(4-trifluoromethylphenyl)-1-(2'-pyridyl)imidazolin-2-ylidene)tricarbonyl-thiocyanato rhenium(I) (**4**): To a flask equipped with a reflux condenser was added **2** (0.050 g, 0.078 mmol), NaSCN (0.633 g, 7.82 mmol), and ethanol:water (22 ml, 1:1 v/v). The mixture was degassed with N_2 for 15 minutes and then refluxed under N_2 for 12 hours in the dark. Then the reaction mixture was cooled to room temperature and extracted with dichloromethane (×3). The combined organic layers were washed with water and dried with Na_2SO_4. Dichloromethane was removed under reduced pressure, and the resultant crude product was purified by silica gel chromatography using 10% ethyl acetate:dichloromethane as the

eluent to give yellow solid **4** (31 mg, 65%). ^{1}H NMR (300 MHz, $CDCl_3$) δ 8.89 (d, *J* = 5.1 Hz, 1H), 8.17 (t, *J* = 7.2 Hz, 1H), 7.92 (d, *J* = 9.0 Hz, 2H), 7.79-7.69 (m, 4H), 7.46 (t, *J* = 4.8 Hz, 1H), 7.37 (s, 1H) ppm. ^{13}C NMR (125 MHz, CD_3CN) δ 195.6, 194.9, 190.2, 189.7, 153.8, 153.2, 142.6, 142.4, 131.1 (ap d, $J_{2\ C\text{-}F}$ = 32.5 Hz), 127.5 (2 C signals), 127.1 (q, $J_{3\ C\text{-}F}$ = 3.8 Hz), 124.9, 124.6, 123.9 (ap d, $J_{1\ C\text{-}F}$ = 270.0 Hz), 118.1, 113.3 ppm. ^{19}F (300 MHz, $CDCl_3$) -63.15 ppm. IR (neat, cm^{-1}) 3010, 2923, 2840, 2101, 2021, 1906, 1614. HRMS (ESI) m/z calculated for $C_{19}H_{10}F_3N_4O_3ReSCs$ ($[M+Cs]^+$) 750.9036, found 750.9026.

Fac-(3-(4-trifluoromethylphenyl)-1-(2'-pyridyl)imidazolin-2-ylidene}tricarbonylacetonitrilerhenium(I) hexafluorophosphonate (**5**): To a flame dried flask equipped with a reflux condenser was added **2** (0.050 g, 0.078 mmol), $AgClO_4.xH_2O$ (0.018 g, 0.081 mmol), and anhydrous acetonitrile (13 ml). The mixture was refluxed under N_2 for 8 hours in the dark. Then the reaction mixture was cooled to room temperature and 1.0 ml of saturated aqueous NH_4PF_6 was added. The solvent volume was reduced under vacuum until solids began to precipitate, and then the mixture was dissolved in 5 ml of an acetone:ethanol:H_2O (1:1:1 v/v/v) mixture. The majority of the solvent was then removed under vacuum to give a light yellow precipitate (**5**) which was collected via vacuum filtration (50 mg, 86%). ^{1}H NMR (300 MHz, $CDCl_3$) δ 8.76 (d, *J* = 4.8 Hz, 1H), 8.25 (t, *J* = 7.8 Hz, 1H), 8.03-7.98 (m, 2H), 7.90 (d, *J* = 8.4 Hz, 2H), 7.74 (d, *J* = 7.8 Hz, 2H), 7.46 (t, *J* = 7.2 Hz, 1H), 7.40 (s, 1H), 2.25 (s, 3H) ppm. ^{13}C NMR (125 MHz, $CDCl_3$) δ 194.1, 192.0, 188.9, 187.1, 153.6, 153.1, 142.9, 141.7, 132.5 (q, $J_{2C\text{-}F}$ = 33.0 Hz), 127.4 (ap d, $J_{3C\text{-}F}$ = 3.6 Hz), 127.0, 124.9, 124.6, 123.3, 123.3 (ap d, $J_{1\ C\text{-}F}$ = 270.9 Hz), 118.9, 114.2, 3.3 ppm. ^{19}F (400 MHz, $CDCl_3$) -64.20 (d, $J_{1\ P\text{-}F}$ = 756 Hz) ppm. The CF_3 signal is predicted to be very close in chemical shift to one to the PF_6 peaks and is not reported. IR (neat, cm^{-1}) 3673, 3175, 3150, 2034, 1922, 1617. HRMS (ESI) m/z calculated for $C_{20}H_{13}F_3N_4O_3Re$ ($[M\text{-}PF_6]^+$) 601.0498, found 601.0497.

Synthesis of *fac-(3-(4-trifluoromethylphenyl)-1-(2'-pyridyl)imidazolin-2-ylidene}tricarbonyltriethyl phosphiterhenium(I) hexafluorophosphonate* (**6**): To a flame dried flask equipped with a reflux condenser was added **2** (0.050 g, 0.078 mmol), $AgSO_3CF_3$ (0.020 g, 0.079 mmol), and dry THF (8 ml). The mixture was refluxed under N_2 for 2 hours in the dark. Then, the resultant solution was transferred into another flask under N_2 while passing through a syringe equipped with a 0.45 µm syringe filter to remove the AgBr precipitate. Then, triethyl phosphite (0.13 ml, 0.782 mmol) was added into the filtered solution, and the mixture was refluxed overnight under N_2 in the dark. The reaction mixture was cooled to room temperature, and THF was removed under reduced pressure. The resultant yellow oil was washed with 2 ml portions of pentane (×5) to remove excess $P(OEt)_3$ to give a yellow solid. The yellow solid was dissolved in methanol (5 ml), and a saturated methanolic solution of NH_4PF_6 (2 ml) was added to the rhenium complex solution. Methanol was removed under reduced pressure. The resultant solid was dissolved in dichloromethane, and the dichloromethane soluble components were concentrated under vacuum. The final pale yellow solid was washed with 2 ml portions of diethyl ether (×5) to remove any residual $P(OEt)_3$ to give **6** (40 mg, 59%). ^{1}H NMR (300 MHz, $CDCl_3$) δ 8.70 (d, *J* = 5.6 Hz, 1H), 8.46 (s, 1H), 8.35-8.30 (m, 2H), 7.90 (d, *J* = 8.4 Hz, 2H), 7.70 (d, *J* = 8.3 Hz, 2H), 7.48 (d, *J* = 2.2 Hz, 1H), 7.40 (p, *J* = 5.1 & 1.8 Hz, 1H), 3.76 (p, *J* = 7.1 Hz, 6H), 1.10 (t, *J* = 7.0 Hz, 9H) ppm. ^{13}C NMR (125 MHz, $CDCl_3$) δ 193.9 (d, $J_{1\ P\text{-}C}$ = 12.5 Hz), 191.4 (d, $J_{1\ P\text{-}C}$ = 12.6 Hz), 186.8 (d, $J_{2\ C\text{-}P}$ = 84.0 Hz), 184.7 (d, $J_{1\ C\text{-}P}$ = 16.4 Hz), 153.4, 153.2, 143.0, 141.6, 132.5 (q, $J_{2\ C\text{-}F}$ = 33.1 Hz), 127.3 (q, $J_{3\ C\text{-}F}$ = 3.5 Hz), 126.7, 125.5, 124.3, 123.3 (ap d, $J_{1\ C\text{-}F}$ = 271.0 Hz), 119.6, 114.6, 62.6 (d, d, $J_{2\ C\text{-}P}$ = 7.3 Hz), 15.9 (d, $J_{3\ C\text{-}P}$ = 5.8 Hz). ^{19}F (400 MHz, $CDCl_3$) -64.54 (d, $J_{1\ P\text{-}F}$ = 756 Hz) ppm. The CF_3 signal is predicted to be very close in chemical shift to one to the PF_6 peaks and is not reported. IR (neat, cm^{-1}) 3200, 3148, 2988, 2965, 2040, 1959, 1930, 1616. HRMS (ESI) m/z calculated for $C_{24}H_{25}F_3N_3O_6PRe$ ($[M\text{-}PF_6]^+$) 726.0992, found 726.0831.

Photocatalysis general procedure. To a 17 ml Pyrex test tube was added BIH (0.005 g, 0.02 mmol), MeCN (6.0 ml), and catalyst (0.2 ml of a 1 × 10^{-3} M MeCN solution). The solution was bubbled vigorously with CO_2 for ~15 minutes until the solution volume reached 1.9 ml. N_2 degassed trimethylamine (0.1 ml) was added to the reaction mixture, and the reaction was sealed with a rubber septum followed by irradiated with a solar simulator. Headspace samples were taken at 20, 40, 60, 120, and 240 minutes.

Computational Details. Density functional theory (DFT) has been used to compute optimized structures, harmonic vibrational frequencies, and electronic energies for the Re(pyNHC-Ph)$(CO)_3$X complexes and dissociation products, with dissociating ligand "X" as Br^-, Cl^-, NCS^-, MeCN, $P(OEt)_3$, or $P(OMe)_3$, where pyNHC-Ph is a simplified model of the pyNHC-PhCF_3 ligand constructed by replacing the CF_3 group by an H atom. Then, electronic dissociation energies D_e were calculated by comparing the electronic energies of the fully coordinated 19 e^- complex to those of the isolated ligand and penta-coordinated 17 e^- complex. The D_e values were also corrected for the zero-point vibrational energies of the species obtained from unscaled harmonic vibrational frequencies to give D_0. Additional computations were performed to determine D_e and D_0 for the dissociation of Br^- from Br-Re(bpy)$(CO)_3$. M06-2X[26] and density-fitted M06-L[27] were used for these computations, with effects of the acetonitrile solvent included by the polarizable continuum model (PCM)[28] for all computations. The integral equation formalism and default solvent parameters for acetonitrile were used for the PCM calculations. For the geometry optimizations and vibrational frequency computations of the ligands and complexes, a double-ζ correlation consistent basis set augmented with diffuse functions on all atoms and a relativistic pseudopotential for the Re center was used (aug-cc-pVDZ-PP).[29-33] After confirming that each M06-2X and M06-L optimized structure was a minimum (no imaginary frequencies), electronic energies were then computed for these structures with an analogous triple-ζ basis set (aug-cc-pVTZ-PP).[29-33] A similar level of theory has been used elsewhere to successfully characterization similar rhenium complexes.[34-35] All computations were performed with Gaussian 09 (Rev: E.01)[36] using an ultrafine pruned numerical integration grid with 99 radial shells and 590 angular points per shell and the default threshold of 1*10^{-6} for removing linearly dependent basis functions. For the frequency computation on the largest complex (with the $P(OEt)_3$ ligand) it was necessary to lower the Coupled Perturbed Hartree Fock convergence tolerance to 1*10^{-7} - maximum change in the U matrix.

Acknowledgements

HPS, NL, and JHD thank NSF for award CHE-1800281 which supported the synthesis, CVs, absorption spectroscopy, and catalytic studies. LEM and NIH thank NSF for award OIA-1539035 which supported the excited-state lifetime studies. TS, CZP, and GST thank NSF for awards OIA-1430364 and CHE-1664998. CZP, JHD, NIH, and GST thank NSF for REU support under award CHE-1757888.

Keywords: Photocatalysis • Reduction • CO_2 • Dissociation • Lifetime

[1] M. Robert, *ACS Energy Lett.* **2016**, *1*, 281-282.
[2] M. Aresta, A. Dibenedetto, A. Angelini, *Chem. Rev.* **2014**, *114*, 1709-1742.
[3] M. Mikkelsen, M. Jørgensen, F. C. Krebs, *Energy Environ. Sci.* **2010**, *3*, 43-81.
[4] J. Hawecker, J.-M. Lehn, R. Ziessel, *J. Chem. Soc. Chem. Commun.* **1983**, 536-538.
[5] C. A. Carpenter, P. Brogdon, L. E. McNamara, G. S. Tschumper, N. I. Hammer, J. H. Delcamp, *Inorganics* **2018**, *6*, 22.
[6] A. J. Huckaba, E. A. Sharpe, J. H. Delcamp, *Inorg. Chem.* **2016**, *55*, 682-690.
[7] S. Sato, T. Morikawa, *ChemPhotoChem* **2017**.

[8] H. Rao, J. Bonin, M. Robert, *Chem. Commun.* **2017**, *53*, 2830-2833.
[9] S. Sato, T. Morikawa, T. Kajino, O. Ishitani, *Angew. Chem. Int. Ed.* **2013**, *52*, 988-992.
[10] A. Genoni, D. N. Chirdon, M. Boniolo, A. Sartorel, S. Bernhard, M. Bonchio, *ACS Catal.* **2016**, 154-160.
[11] P. V. Simpson, M. Falasca, M. Massi, *Chem. Commun.* **2018**, *54*, 12429-12438.
[12] H. Takeda, K. Koike, H. Inoue, O. Ishitani, *J. Am. Chem. Soc.* **2008**, *130*, 2023-2031.
[13] C. Bruckmeier, M. W. Lehenmeier, R. Reithmeier, B. Rieger, J. Herranz, C. Kavakli, *Dalton. Trans.* **2012**, *41*, 5026-5037.
[14] J. G. Vaughan, B. L. Reid, S. Ramchandani, P. J. Wright, S. Muzzioli, B. W. Skelton, P. Raiteri, D. H. Brown, S. Stagni, M. Massi, *Dalton. Trans.* **2013**, *42*, 14100-14114.
[15] T. Mukuta, P. V. Simpson, J. G. Vaughan, B. W. Skelton, S. Stagni, M. Massi, K. Koike, O. Ishitani, K. Onda, *Inorg. Chem.* **2017**, *56*, 3404-3413.
[16] P. Kurz, B. Probst, B. Spingler, R. Alberto, *Eur. J. Inorg. Chem.* **2006**, *2006*, 2966-2974.
[17] N. P. Liyanage, H. A. Dulaney, A. J. Huckaba, J. W. Jurss, J. H. Delcamp, *Inorg. Chem.* **2016**, *55*, 6085-6094.
[18] J. G. Vaughan, B. L. Reid, P. J. Wright, S. Ramchandani, B. W. Skelton, P. Raiteri, S. Muzzioli, D. H. Brown, S. Stagni, M. Massi, *Inorg. Chem.* **2014**, *53*, 3629-3641.
[19] R. R. Rodrigues, C. M. Boudreaux, E. T. Papish, J. H. Delcamp, *ACS Appl. Energy Mater.* **2019**, *2*, 37-46.
[20] C. M. Boudreaux, N. P. Liyanage, H. Shirley, S. Siek, D. L. Gerlach, F. Qu, J. H. Delcamp, E. T. Papish, *Chem. Commun.* **2017**, *53*, 11217-11220.
[21] S. Das, R. R. Rodrigues, R. W. Lamb, F. Qu, E. Reinheimer, C. M. Boudreaux, C. E. Webster, J. H. Delcamp, E. T. Papish, *Inorg. Chem.* **2019**, *58*, 8012-8020.
[22] C. J. Stanton, 3rd, C. W. Machan, J. E. Vandezande, T. Jin, G. F. Majetich, H. F. Schaefer, 3rd, C. P. Kubiak, G. Li, J. Agarwal, *Inorg. Chem.* **2016**, *55*, 3136-3144.
[23] J. Agarwal, T. W. Shaw, C. J. Stanton, 3rd, G. F. Majetich, A. B. Bocarsly, H. F. Schaefer, 3rd, *Angew. Chem. Int. Ed.* **2014**, *53*, 5152-5155.
[24] C. J. Stanton, 3rd, J. E. Vandezande, G. F. Majetich, H. F. Schaefer, 3rd, J. Agarwal, *Inorg. Chem.* **2016**, *55*, 9509-9512.
[25] Y. Kuramochi, O. Ishitani, H. Ishida, *Coord. Chem. Rev.* **2018**, *373*, 333-356.
[26] Y. Zhao, D. G. Truhlar, *Theor. Chem. Acc.* **2008**, *120*, 215-241.
[27] Y. Zhao, D. G. Truhlar, *J. Chem. Phys.* **2006**, *125*, 194101.
[28] J. Tomasi, B. Mennucci, R. Cammi, *Chem. Rev.* **2005**, *105*, 2999-3093.
[29] D. Figgen, K. A. Peterson, M. Dolg, H. Stoll, *J. Chem. Phys.* **2009**, *130*, 164108.
[30] T. H. Dunning, *J. Chem. Phys.* **1989**, *90*, 1007-1023.
[31] R. A. Kendall, T. H. Dunning, R. J. Harrison, *J. Chem. Phys.* **1992**, *96*, 6796-6806.
[32] A. K. Wilson, D. E. Woon, K. A. Peterson, T. H. Dunning, *J. Chem. Phys.* **1999**, *110*, 7667-7676.
[33] D. E. Woon, T. H. Dunning, *J. Chem. Phys.* **1993**, *98*, 1358-1371.
[34] J. Agarwal, E. Fujita, H. F. Schaefer, 3rd, J. T. Muckerman, *J. Am. Chem. Soc.* **2012**, *134*, 5180-5186.
[35] J. Agarwal, R. P. Johnson, G. Li, *J. Phys. Chem. A* **2011**, *115*, 2877-2881.
[36] M. J. Frisch, G. W. Trucks, H. B. Schlegel, G. E. Scurseria, M. A. Robb, J. R. Cheeseman, G. Scalmani, V. Barone, B. Mennucci, A. Petersson, H. Nakatsuji, M. Caricato, X. Li, H. P. Hratchian, A. F. Izmaylov, J. Bloino, G. Zheng, J. L. Sonnenberg, M. Hada, M. Ehara, K. Toyota, R. Fukuda, J. Hasegawa, M. Ishida, T. Nakajima, Y. Honda, O. Kitao, H. Nakai, t. Vreven, J. A. Montgomery Jr., J. E. Peralta, F. Ogliaro, M. Bearpark, J. J. Heyd, E. Brothers, K. N. Kudin, V. N. Staroverov, R. Kobayashi, J. Normand, K. Raghavachari, A. Rendell, J. C. Burant, S. S. Iyengar, J. Tomasi, M. Cossi, N. Rega, J. M. Millam, M. Klene, J. E. Knox, J. B. Cross, V. Bakken, C. Adamo, J. Jaramillo, R. Gomperts, R. E. Stratmann, O. Yazyev, A. J. Austin, R. Cammi, C. Pomelli, J. W. Ochterski, R. L. Martin, K. Morokuma, V. G. Zakrzewski, G. A. Voth, P. Salvador, J. J. Dannenberg, S. Dapprich, A. D. Daniels, O. Farkas, J. B. Foresman, J. V. Ortiz, J. Cioslowski, D. J. Fox, *Gaussian, Inc.* **2009**, *Wallingford, CT, USA*, Gaussian09 Revision E.01.

Entry for the Table of Contents

Insert graphic for Table of Contents here.

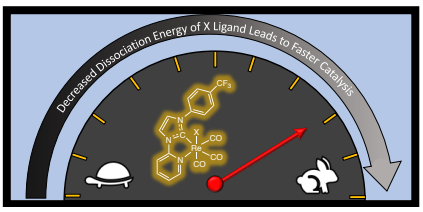

An in-depth look at a series of rhenium-based photocatalysts with a pyridyl-NHC ligand framework that facilitate the reduction of CO_2 to CO. The importance of selecting an appropriate “X” ligand is described through detailed photocatalytic, electrochemical, photophysical, computational, and excited-state lifetime studies which reveal a weakly binding "X" ligand is key to catalysis.

Institute and/or researcher Twitter usernames: @Olemissrebels @DelcampGroup

Key Topic: Photocatalysis